

1 *Conference Proceedings Paper*

2 **Attainment of Pentagonal-Bipyramidal Ln^{III}** 3 **Complexes from a Planar Pentadentate Ligand**

4 **Julio Corredoira-Vázquez, Matilde Fondo, Jesús Sanmartín-Matalobos and Ana M.**
5 **García-Deibe***

6 Departamento de Química Inorgánica . Facultade de Química. Campus Vida. Universidade de Santiago de
7 Compostela. Santiago de Compostela. 15782 SPAIN. julio_corredoira@hotmail.com (J.C.-V.);
8 matilde.fondo@usc.es (M.F.); jesus.sanmartin@usc.es (J.S.-M.); ana.garcia.deibe@usc.es (A.M.G.-D.)

9 * Correspondence: ana.garcia.deibe@usc.es; Tel.: +34-981814237

10 Received: date; Accepted: date; Published: date

11 **Abstract:** The search for mononuclear lanthanoid-based single-ion magnets (SIMs) has increased
12 the interest in some coordination environments with low coordination numbers, in combination
13 with an axial symmetry, as they could maximize the anisotropy of complexes of oblate lanthanoid
14 ions, as dysprosium(III). In this sense, the pentagonal-bipyramid geometry can have ground-state
15 doublets with perfect axiality, and therefore such complexes can be good candidates for SIMs. In
16 our particular case, we have used a well-known open planar pentadentate chelating Schiff base
17 ligand as 2,6-bis(1-salicyloylhydrazonoethyl)pyridine) (H₄daps) for the synthesis of air-stable
18 pentagonal-bipyramidal Ln^{III} complexes (being Ln: Dy and Er, oblate and prolate, respectively), in
19 order to compare their structures. Thus, reaction of H₄daps with (CH₃)₄NOH·5H₂O, and the
20 corresponding LnCl₃·hexahydrate has yielded heptacoordinate [(CH₃)₄N][Ln^{III}(H₂daps)Cl₂]
21 complexes, where the tetramethylammonium cation is acting as counterion of
22 pentagonal-bipyramidal Ln^{III} complexes, which are bearing two chloride atoms in apical positions.
23 As both complexes could be crystallized as single crystals, we can compare their crystal structures,
24 as well as with other related complexes in literature, but containing different counterions, trying to
25 see their influence on other properties of the compounds, as their magnetic behavior.

26 **Keywords:** Lanthanoid; dysprosium(III); erbium(III); pentagonal-bipyramidal coordination
27 environment; pentadentate ligand; hydrazone; Schiff base
28

29 **1. Introduction**

30 Since the discovery of the first single-ion magnet (SIM) in 2003 [1], and the realization that the
31 control of anisotropy is the key factor for the isolation of single molecule magnets (SMMs), the field
32 of molecular magnetism began to focus on the lanthanoid elements, since they present intrinsic
33 anisotropy. However, the anisotropy of the whole molecule is modulated by the interaction between
34 the single-ion electron density and the crystal field environment in which it is placed, as Reinhart
35 and Long have predicted [2]. In this sense, for oblate ions a strong axial crystal field should
36 maximize the uniaxial anisotropy, while for prolate ions, a strong crystal field in the equatorial plane
37 is preferable. Accordingly, dysprosium should maximize its anisotropy in a lineal environment.³
38 However, lanthanoids hardly stabilize the coordination number 2, unless with very bulky ligands, as
39 occurring in metallocenes, which are holding the record of blocking temperature (80 K) [3], although
40 they are not air stable.

41 In the absence of air stable complexes with coordination number 2, the coordination number 7,
42 with pentagonal bipyramidal (pbp) geometry, was the most explored one, leading to the blocking

43 temperature record for an air-stable complex of 20 K [4]. Therefore, in order to improve the magnetic
44 behaviour of this kind of complexes, more research is still needed in this area. With these
45 considerations in mind, in this study we will describe the synthesis and magnetic characterization of
46 a dysprosium and an erbium complex with pbp geometry derived from a well-known planar
47 pentadentate donor.

48 2. Materials and Methods

49 All chemical reagents were purchased from commercial sources and used as received without
50 further purification. Elemental analyses of C, H and N were performed on a Carlo Erba EA 1108
51 analyzer. Infrared spectra were recorded in the ATR mode on a Varian 670 FT/IR spectrophotometer
52 in the range 4000-500 cm^{-1} . ^1H NMR spectra of 2,6-bis(1-salicyloylhydrazonoethyl)pyridine (H_4daps)
53 was recorded on a Bruker DPX-250 spectrometer.

54 H_4daps was obtained by a variation of a previously described method [5], using methanol as
55 solvent instead of benzene, and it was satisfactorily characterized by ^1H NMR spectroscopy.

56 2.1. Syntheses of the complexes

57 Both $(\text{CH}_3)_4\text{N}[\text{Ln}(\text{H}_2\text{daps})\text{Cl}_2]$ ($\text{Ln} = \text{Dy}, \text{Er}$) complexes were obtained in the same way, which is
58 exemplified by the isolation of $(\text{CH}_3)_4\text{N}[\text{Dy}(\text{H}_2\text{daps})\text{Cl}_2]$ (**DyH₂daps**): To a suspension of H_4daps
59 (0.100 g, 0.232 mmol) in THF (25 mL), $(\text{CH}_3)_4\text{NOH}\cdot 5\text{H}_2\text{O}$ (0.087 g, 0.463 mmol) and 27 mL of CH_3CN
60 are added. The mixture is stirred for 30 min at 35 °C, and a yellow solution was obtained.
61 $\text{DyCl}_3\cdot 6\text{H}_2\text{O}$ (0.087 g, 0.232 mmol) was added to the solution, and the new mixture was stirred for 4 h
62 at room temperature. The resulting solution was concentrated up to half of its volume, and
63 evaporation of this concentrated solution yields single crystals of $(\text{CH}_3)_4\text{N}[\text{Dy}(\text{H}_2\text{daps})\text{Cl}_2]$ after 24 h.
64 The crystals were filtered and dried in air. Yield: 0.125 g (73%). Elemental analysis calcd. for
65 $\text{C}_{27}\text{H}_{31}\text{Cl}_2\text{DyN}_6\text{O}_4$ (736.98): C, 43.96; N 11.40; H 4.21%. Found: C, 43.25; N, 11.39; H, 4.85%. IR (ATR,
66 $\tilde{\nu}/\text{cm}^{-1}$): 1594 (amide I), 1523 (amide II), 3363 (OH).

67 $(\text{CH}_3)_4\text{N}[\text{Er}(\text{H}_2\text{daps})\text{Cl}_2]$ (**ErH₂daps**): quantity of $\text{ErCl}_3\cdot 6\text{H}_2\text{O}$ (0.088 g, 0.232 mmol). Single
68 crystals of $(\text{CH}_3)_4\text{N}[\text{Er}(\text{H}_2\text{daps})\text{Cl}_2]$ are obtained in the same way as those of **DyH₂daps**. Yield: 0.036
69 g (21%). Elemental analyses calcd. for $\text{C}_{27}\text{H}_{31}\text{Cl}_2\text{ErN}_6\text{O}_4$ (741.74): C, 43.68; N 11.32; H 4.18%. Found: C,
70 43.36; N, 11.36; H, 4.75%. IR (ATR, $\tilde{\nu}/\text{cm}^{-1}$): 1586 (amide I), 1521 (amide II), 3367 (OH)

71 2.1. X-ray studies

72 Single crystals of $(\text{CH}_3)_4\text{N}[\text{Dy}(\text{H}_2\text{daps})\text{Cl}_2]$ and $(\text{CH}_3)_4\text{N}[\text{Er}(\text{H}_2\text{daps})\text{Cl}_2]$ were obtained as
73 detailed above. Data were collected at 225 K on a Bruker Kappa APEXII CCD diffractometer,
74 employing graphite monochromatized Mo- $\text{K}\alpha$ ($\lambda = 0.71073 \text{ \AA}$) radiation. Multi-scan absorption
75 corrections were applied using SADABS [6]. These structures were solved by standard direct
76 methods, employing SHELXT [7], and then refined by full-matrix least-squares techniques on F^2 ,
77 using SHELXL [8] from the program package SHELX-2014 [9]. Main crystal data are presented in
78 Table 1.

79 All non-hydrogen atoms corresponding to the cationic complexes were anisotropically refined.
80 Hydrogen atoms were typically included in the structure factor calculations in geometrically
81 idealized positions. In contrast, those hydrogen atoms attached to oxygen and/or nitrogen atoms of
82 the ligands were found in the corresponding Fourier maps, and then either they were freely refined,
83 or with thermal parameters derived from the parent atoms.

84 Powder diffractograms of **DyH₂daps** and **ErH₂daps** were recorded in a Philips diffractometer
85 with a PW1710 control unit, a vertical PW1820/00 goniometer and an Enraf Nonius FR590 generator,
86 operating at 40 kV and 30 mA, using monochromatized Cu- $\text{K}\alpha$ ($\lambda = 1.5418 \text{ \AA}$) radiation. A scan was
87 performed in the range $5 < 2\theta < 28.5^\circ$ with $t = 10 \text{ s}$ and $\Delta 2\theta = 0.02^\circ$. LeBail refinement was obtained
88 with the aid of HighScore Plus Version 3.0d.

89
90

91 **Table 1.** Crystal data and structure refinement for **DyH₂daps** and **ErH₂daps**

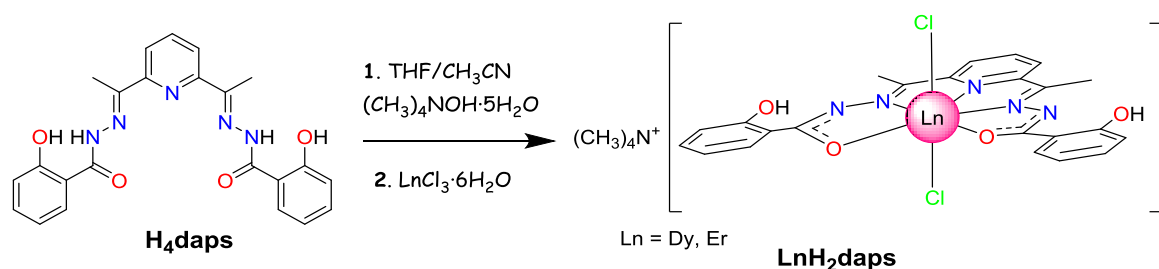
	(CH ₃) ₄ N[Dy(H ₂ daps)Cl ₂]	(CH ₃) ₄ N[Er(H ₂ daps)Cl ₂]
Formula	C ₂₇ H ₃₁ Cl ₂ DyN ₆ O ₄	C ₂₇ H ₃₁ Cl ₂ ErN ₆ O ₄
M.W.	736.98	741.74
Temperature (K)	225(2)	250(2)
Crystal system	Orthorhombic	Orthorhombic
Space group	<i>C m c 2</i> ₁	<i>C m c 2</i> ₁
<i>a</i> (Å)	17.8879(9)	17.8142(18)
<i>b</i> (Å)	14.3964(7)	14.5177(14)
<i>c</i> (Å)	12.2189(6)	12.1790(14)
Volume (Å ³)	3146.6(3)	3149.7(6)
<i>Z</i>	4	4
Absorp. Coef. (mm ⁻¹)	2.585	2.874
Reflections collected	28494	17722
Independent reflections	3529 [<i>R</i> _{int} = 0.0353]	4710 [<i>R</i> _{int} = 0.0391]
Data / restraints / param.	3529 / 1 / 200	4710 / 1 / 201
Final <i>R</i> indices [<i>I</i> > 2σ(<i>I</i>)]	<i>R</i> ₁ = 0.0268, <i>wR</i> ₂ = 0.0534	<i>R</i> ₁ = 0.0327, <i>wR</i> ₂ = 0.0654
<i>R</i> indices (all data)	<i>R</i> ₁ = 0.0328, <i>wR</i> ₂ = 0.0560	<i>R</i> ₁ = 0.0420, <i>wR</i> ₂ = 0.0691

92 **2.2. Magnetic measurements**

93 Magnetic susceptibility dc and ac measurements for powder crystalline samples of **DyH₂daps**
 94 and **ErH₂daps** were carried out with a Quantum Design SQUID MPMS-XL susceptometer. The
 95 magnetic susceptibility data were recorded under magnetic fields of 1000 Oe in the range 2-300 K.
 96 Magnetization measurements at 2.0 K were recorded under magnetic fields ranging from 0 to
 97 50000 Oe. Diamagnetic corrections were estimated from Pascal's Tables. Alternating current (ac)
 98 susceptibility measurements in different applied static fields (*H*_{ac} = 0 or 1000) were performed with
 99 an oscillating ac field of 4 Oe and ac frequency of 1400 Hz for both complexes. In the case of
 100 **DyH₂daps**, ac susceptibility measurements were additionally recorded under a dc field of 1000 Oe at
 101 ac frequencies ranging from 10 to 1488 Hz.

102 **3. Results and discussion**

103 The complexes (CH₃)₄N[Ln(H₂daps)Cl₂] (Ln = Dy, Er) were obtained as summarized in
 104 Scheme 1. Thus, the reaction of a suspension of H₄daps in THF with tetramethylammonium
 105 hydroxide, followed by the addition of LnCl₃·6H₂O at room temperature gave rise to a yellow
 106 solution that, after concentration and slow evaporation, yielded single crystals of the **LnH₂daps**,
 107 which resulted to be suitable for X-ray diffraction studies. This method of isolation of the complexes
 108 differs from that previously reported for (CH₃CH₂)₃NH[Ln(H₂daps)Cl₂] (Ln = Tb, Dy) [10], since in
 109 our case the syntheses were carried out using less solvent at room temperature instead of reflux, but
 110 with an improved yield (73% compared to 64% for related (CH₃CH₂)₃NH[Dy(H₂daps)Cl₂]).
 111



112

113

Scheme 1. Reaction scheme for the isolation of complexes **LnH₂daps**

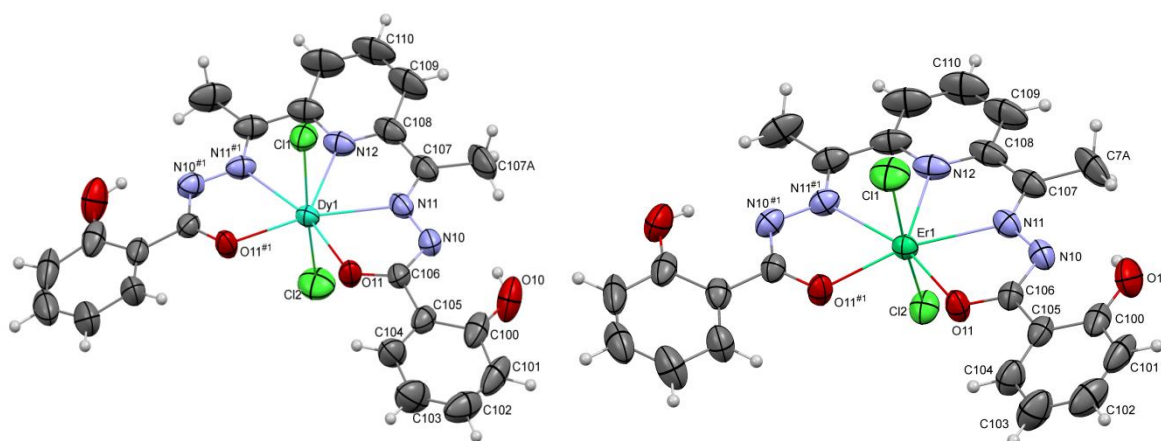
114 The complexes could be unequivocally characterized by elemental analysis, IR spectroscopy,
115 and by X-ray diffraction techniques, and their magnetic behavior was also analyzed.

116 The infrared spectra of the compounds show two intense bands at *ca.* 1590 and 1520 cm⁻¹, which
117 can be assigned to the amide I [$\nu(\text{C}=\text{O})$] and the amide II [$\delta(\text{NH}) + \nu(\text{C}=\text{N})$] vibrations, respectively
118 [5,11-13]. These bands experience significant negative shifts ranging from 30 to 65 cm⁻¹ with respect
119 to free H₂daps, what is consistent with the coordination of both carbonyl and both imine groups to
120 the metal centers [5,10-13]. The spectra also show the presence of a quite broad band centered at
121 about 3360 cm⁻¹, which can be assigned to OH vibrations, in agreement with the non-deprotonation
122 of the phenolic groups.

123 3.1. Crystal structures

124 Despite multiple attempts to record the data and solve the structures of both complexes at a
125 lower temperature of 100 K, these processes resulted to be unsuccessful, so they were finally
126 recorded at 225 and 250 K. The reason for this problem appears to be related with modulated crystal
127 structures [14], what avoids a satisfactory solution at low temperature, even using disorder models
128 which mostly affect to the (CH₃)₄N⁺ counterion.

129 The structures of both compounds at 225 and 250 K are highly similar, as ellipsoid diagrams
130 shown in Figure 1 demonstrate. Main bond distances and angles are summarized in table 2. Their
131 crystal structures are also very similar to those described for Et₃NH[M(H₂daps)Cl₂] (M = Tb, Dy and
132 Y) complexes [10].



133

134 **Figure 1.** Ellipsoids diagram (50% probability) for [Dy(H₂daps)Cl₂]⁻ and [Er(H₂daps)Cl₂]⁻ anions in
135 **DyH₂daps** and **ErH₂daps**. The (CH₃)₄N⁺ counterions have been omitted for clarity.

136

Table 2. Main bond distances (Å) and angles (°) for **DyH₂daps** and **ErH₂daps**

Dy1-O11	2.253(4)	Er1-O11	2.238(4)
Dy1-N12	2.426(8)	Er1-N12	2.418(8)
Dy1-N11	2.449(5)	Er1-N13	2.426(5)
Dy1-Cl2	2.613(2)	Er1-Cl1	2.585(3)
Dy1-Cl1	2.623(2)	Er1-Cl2	2.604(3)
Cl2-Dy1-Cl1	171.44(9)	Cl2-Er1-Cl1	171.73(10)
O11 ^{#1} -Dy1-O11	98.94(18)	O11 ^{#1} -Er1-O11	96.36(19)
O11-Dy1-N11	65.38(15)	O11-Er1-N11	66.00(15)
N12-Dy1-N11	65.17(11)	N11-Er1-N12	65.85(12)

137

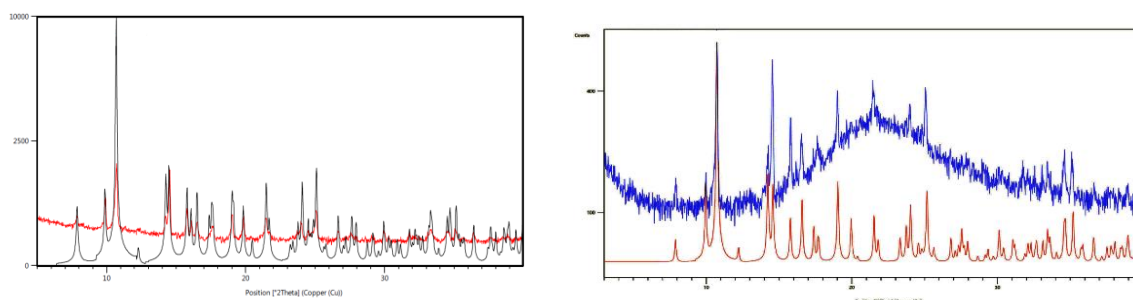
#1

138 Thus, the unit cell of both complexes contain [Ln(H₂daps)Cl₂]⁻ (Ln = Dy or Er) anions and
139 (CH₃)₄N⁺ cations, where two of the CH₃ groups are disordered over two sites. The [Ln(H₂daps)Cl₂]⁻
140 anion is bisected by a crystallographic plane that contains the lanthanoid atom, the chloride ligands
141 and the pyridine nitrogen atom, thus making both halves of the bisdeprotonated H₂daps²⁻ ligand

142 equivalent. This donor acts as pentadentate, using the N_{pyridine}, N_{imine} and O_{carbonyl} atoms to bind the
 143 Ln^{III} ion. Accordingly, H₂daps²⁻ provides an N₃O₂ environment to the metal centre. The coordination
 144 sphere of the lanthanoid atom is completed by two chloride anions. Therefore, the coordination
 145 number for the metal ion is 7, with slightly distorted pentagonal bipyramidal geometry. The N₃O₂
 146 core is nearly in a perfect plane, the main deviation of any atom from the calculated equatorial plane
 147 being of *ca.* 0.035 Å for **DyH₂daps** and 0.044 Å for **ErH₂daps**, the metal centre lying 0.003 (Dy) or 0.01
 148 Å (Er) above the plane. The arrangement of the pentadentate ligand around the metal centre is
 149 reinforced by typical intramolecular H bonds between the phenol moiety and the amine nitrogen
 150 atom N10.

151 In the pseudo pentagonal bipyramid, the angles around the metal ion differ from the ideal
 152 values of 180 and 72°, the main distortion arising from the O-Dy-O angle of the equatorial plane
 153 (98.94(18)° for **DyH₂daps** and 93.36(19)° for **ErH₂daps**). In spite of this, all the distances and angles
 154 are within their normal range [10,13,15], but it should be noted that the Dy-N_{pyridine} distance is a bit
 155 shorter than in related Et₃NH[Dy(H₂daps)Cl₂] [10], and that the Cl-Dy-Cl angle is notably less
 156 deviated from 180 in **DyH₂daps** (171.44(9)°) than in Et₃NH[Dy(H₂daps)Cl₂] (166.32(6)°), showing
 157 that the cationic counterion could have an important influence in the structural parameters of the
 158 anionic complex. This may be related with the N-H...Cl interaction between the Et₃NH⁺ cation and
 159 one of the chloride ligands.

160 Finally, the comparison of the experimental powder X-ray diffractogram of the crystalline
 161 products at room temperature with the calculated ones from single X-ray diffraction data (Fig. 2) at
 162 298 K demonstrates that both products have been obtained with high purity, and that the collected
 163 samples and the solved single crystals are the same compounds, with the same structure.



164

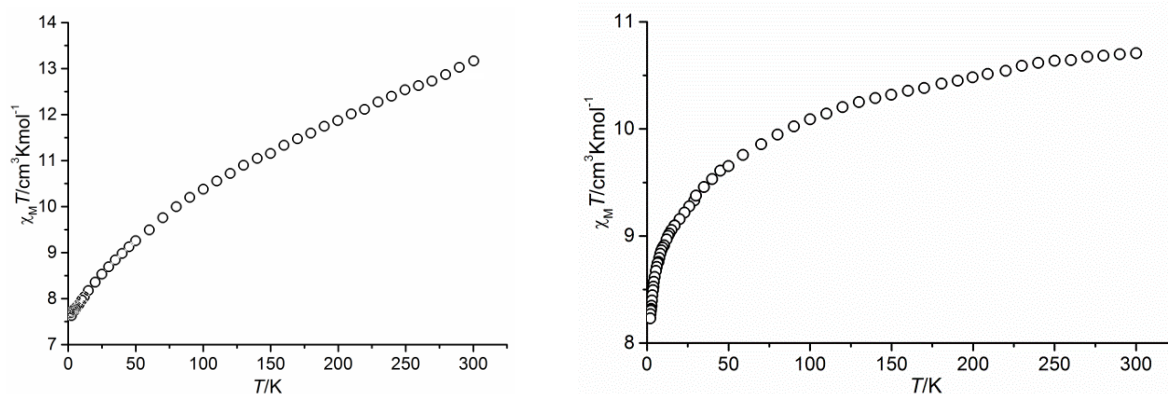
165 **Figure 2.** X-ray powder diffraction for: left) **DyH₂daps** (red) and simulation from single X-ray data at
 166 225 K (black); right) **ErH₂daps** (blue) and simulation from single X-ray data at 250 K (red).

167 3.2. Magnetic Properties

168 Direct-current (dc) magnetic susceptibility measurements were recorded for **DyH₂daps** and
 169 **ErH₂daps**. The plot for χ_{MT} vs T for **DyH₂daps** is shown in Fig. 3, as an example. At 300 K, the χ_{MT} vs
 170 T is 13.1 cm³Kmol⁻¹, a value similar but a bit lower than that expected for one isolated Dy³⁺ ion. This
 171 led to attempts to record the magnetic data newly, what allowed discovering that the magnetic data
 172 were not reproducible, in spite of the high purity of the sample. This seems to be related with the
 173 changes in the crystal structure below 225 K. Thus, the fresh sample, if it is measured from 300 to
 174 2 K, gives a χ_{MT} vs T curve which differs with that recorded from 2 to 300 K, or from the one
 175 recorded from 300 to 2 K once the sample was previously cooled to 2 K. And the same phenomenon
 176 was also observed for **ErH₂daps**.

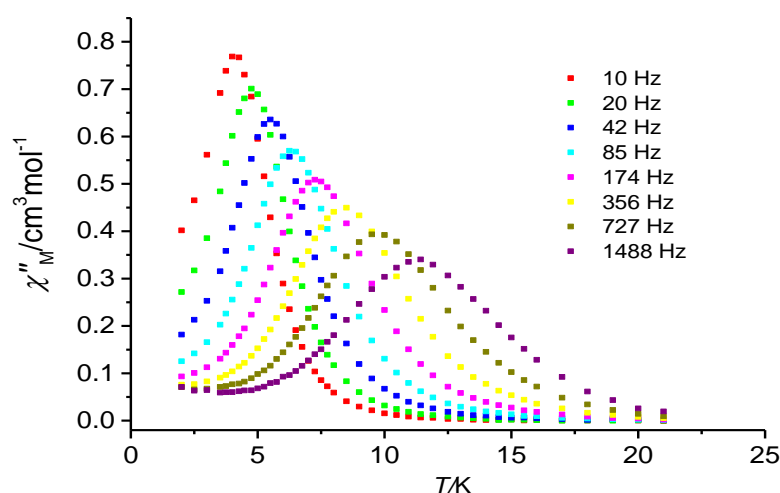
177 Despite this disadvantage that does not allow an accurate interpretation of the magnetic results,
 178 ac magnetic measurements were recorded in order to know the potentiality of these complexes as
 179 molecular magnets. Thus, alternating current (ac) magnetic susceptibility measurements were
 180 initially recorded under a zero external field at a frequency of 1400 Hz. In this case, none of the
 181 compounds show out-of-phase ac susceptibilities (χ''_M) peaks. However, in the presence of an
 182 applied field of 1000 Oe, **ErH₂daps** still lacks χ''_M peaks, while **DyH₂daps** shows ac susceptibility

183 frequency and field dependence below 12 K (Fig. 4). Thus, these data reveal that **DyH₂daps** is a
 184 field-induced SIM, while **ErH₂daps** is not.



185

186 **Figure 3.** $\chi_M T$ vs T for **DyH₂daps**: left) a fresh sample, recorded from 300 to 2 K; right) a fresh sample,
 187 recorded from 2 to 300 K.



188

189 **Figure 4.** Temperature dependence of χ''_M for **DyH₂daps** in $H_{dc} = 1000$ Oe at different frequencies

190 Despite the *ac* results for **DyH₂daps**, the data could not be properly analysed, because, as
 191 previously discussed, these data are not completely reproducible, and no more *ac* parameters could
 192 be calculated.

193 4. Conclusions

194 Two pentagonal bipyramidal Dy and Er complexes were obtained with high purity and fully
 195 characterized. The complexes undergo changes in their structures below 225 K, which seem related
 196 to the tetramethylammonium counterion, since such changes had not been described for similar
 197 complexes with triethylammonium counterions. Accordingly, this work demonstrates that it is easy
 198 to obtain pentagonal bipyramidal complexes using H₄daps as a ligand, but that the stability of the
 199 formed anionic complexes seems to depend on the counterion. A rigorous magnetic analysis of the
 200 complexes is hampered by these changes in the structure at low temperature but, in spite of this, *ac*
 201 measurements clearly show that the **DyH₂daps** is a field-induced SIM, while **ErH₂daps** lacks SIM
 202 behaviour even in the presence of an external dc field of 1000 Oe.

203 **Acknowledgments:** Authors thank the Spanish Ministerio de Innovación, Ciencia y Universidades (PGC2018
 204 102052-B-C21) for financial support. J.C.V thanks Xunta de Galicia for his Ph.D. fellowship.

205 **Conflicts of Interest:** The authors declare no conflict of interest.

206 **References**

- 207 1. Ishikawa, N.; Sugita, M.; Ishikawa, T.; Koshihara, S.; Kaizu, Y. Lanthanide double decker complexes
208 functioning as magnets at the single-molecular level. *J. Am. Chem. Soc.* **2003**, *125*, 8694-8695.
209 doi:10.1021/ja029629nv.
- 210 2. Rinehart, J. D.; Long, J. R. Exploiting single-ion anisotropy in the design of f-element single-molecule
211 magnets. *Chem. Sci.* **2011**, *2*, 2078-2085. doi: 10.1039/c1sc00513h.
- 212 3. Guo, F.-S.; Day, B. M.; Chen, Y.-C.; Tong, M.-L.; Mansikkamäki A.; Layfield, R. A. Magnetic hysteresis up
213 to 80 kelvin in a dysprosium metallocene single-molecule magnet, *Science*, **2018**, *362*, 1400-1403. doi:
214 10.1126/science.aav0652
- 215 4. Chen, Y.-C.; Liu, J.-L.; Ungur, L.; Liu, J.; Li, Q.-W.; Wang, L.-F.; Ni, Z.-P.; Chibotaru, L. F.; Chen, X.-M.; Tong,
216 M.-L. Symmetry-supported magnetic blocking at 20 K in pentagonal bipyramidal Dy(III) single-ion
217 magnets, *J. Am. Chem. Soc.*, **2016**, *138*, 2829-2837. doi: 10.1021/jacs.5b13584.
- 218 5. Pelizzi, C.; Pelizzi, G. Investigation into aroylhydrazones as chelating agents. Synthesis and structural
219 characterization of a tin(IV) complex with 2,6 diacetylpyridine bis(salicyloylhydrazone). *J. Chem. Soc.*
220 *Dalton Trans.* **1980**, 1970-1973. doi: 10.1039/DT9800001970
- 221 6. (a) Blessing, R. H. An empirical correction for absorption anisotropy. *Acta Crystallogr., Sect. A: Found.*
222 *Crystallogr.* **1995**, *A51*, 33-38. doi: 10.1107/S0108767394005726 ; (b) Krause, L.; Herbst-Irmer, R.; Sheldrick
223 G. M.; Stalke, D. Comparison of silver and molybdenum microfocus X-ray sources for single- crystal
224 structure determination. *J. Appl. Cryst.* **2015**, *48*, 3-10. doi: 10.1107/S1600576714022985
- 225 7. Sheldrick, G. M. SHELXT - Integrated space-group and crystal-structure determination. *Acta Cryst.* **2015**,
226 *A71*, 3-8. doi: 10.1107/S2053273314026370
- 227 8. Sheldrick, G. M. Crystal structure refinement with SHELXL. *Acta Cryst.* **2015**, *C71*, 3-8.
228 doi.org/10.1107/S2053229614024218.
- 229 9. Sheldrick, G. M. A short history of SHELX. *Acta Cryst.* **2008**, *A64*, 112-122. doi:
230 10.1107/S0108767307043930.
- 231 10. Bar, A. K.; Kalita, P.; Sutter, J.-P. Chandrasekhar, V. Pentagonal-bipyramid Ln(III) complexes exhibiting
232 single-ion-magnet behavior: a rational synthetic approach for a rigid equatorial plane. *Inorg. Chem.* **2018**,
233 *57*, 2398-2401. doi.org/10.1021/acs.inorgchem.8b00059
- 234 11. Bonardi, A.; Merlo, C.; Pelizzi, C.; Pelizzi, G.; Tarasconi, P.; Cavatorta, F. Synthesis, spectroscopic and
235 structural characterization of mono- and binuclear iron(II) complexes with 2,6-diacetylpyridine
236 bis(acylhydrazones). *J. Chem. Soc, Dalton Trans.* **1991**, 1063-1069. doi: 10.1039/DT9910001063
- 237 12. Bermejo, M. R.; Fondo, M.; Gonzalez, A. M.; Hoyos, O. L.; Sousa, A.; McAuliffe, C. A.; Hussain, W.;
238 Pritchard, R.; Novotorsev, V. M. Electrochemical synthesis and structural characterization of transition
239 metal complexes with 2,6-bis(1-salicyloylhydrazonoethyl)pyridine, H4daps. *J. Chem. Soc, Dalton Trans.*
240 **1999**, 2211-2218. doi: 10.1039/A902018G.
- 241 13. Fondo, M.; Corredoira-Vázquez, J.; García-Deibe, A.M.; Sanmartín-Matalobos, J.; Herrera, J. M.; Colacio, E.
242 Tb₂, Dy₂, and Zn₂Dy₄ Complexes Showing the Unusual Versatility of a Hydrazone Ligand toward
243 Lanthanoid Ions: a Structural and Magnetic Study *Inorg. Chem.* **2018**, *57*, 10100-10110. doi:
244 10.1021/acs.inorgchem.8b01251.
- 245 14. Bolotina, N. B. X-ray diffraction analysis of modulated crystals: Review. *Crystallogr. Rep.* **2007**, *52*, 647-658.
246 doi: 10.1134/S1063774507040128
- 247 15. Mondal, A. K.; Goswami, S.; Konar, S. Influence of the coordination environment on slow magnetic
248 relaxation and photoluminescence behavior in two mononuclear dysprosium(III) based single molecule
249 magnets. *Dalton Trans.* **2015**, *44*, 5086-5094. doi: 10.1039/C4DT03620D.



© 2020 by the authors. Submitted for possible open access publication under the terms and conditions of the Creative Commons Attribution (CC BY) license (<http://creativecommons.org/licenses/by/4.0/>).